# Kinetic narrowing of size distribution

V. G. Dubrovskii*

*St. Petersburg Academic University, Khlopina 8/3, 194021 St. Petersburg, Russia;*
*Ioffe Physical Technical Institute of the Russian Academy of Sciences, Politekhnicheskaya 26, 194021 St. Petersburg, Russia;*
*and ITMO University, Kronverkskiy pr. 49, 197101 St. Petersburg, Russia*

(Received 13 January 2016; revised manuscript received 26 April 2016; published 23 May 2016)

We present a model that reveals an interesting possibility for narrowing the size distribution of nanostructures when the deterministic growth rate changes its sign from positive to negative at a certain stationary size. Such a behavior occurs in self-catalyzed one-dimensional III-V nanowires and more generally whenever a negative "adsorption-desorption" term in the growth rate is compensated by a positive "diffusion flux." By asymptotically solving the Fokker-Planck equation, we derive an explicit representation for the size distribution that describes either Poissonian broadening or self-regulated narrowing depending on the parameters. We show how the fluctuation-induced spreading of the size distribution can be completely suppressed in systems with size self-stabilization. These results can be used for obtaining size-uniform ensembles of different nanostructures.

DOI: 10.1103/PhysRevB.93.174203

## I. INTRODUCTION

It is well documented that the size uniformity of nanostructure ensembles strongly enhances their physical properties and is paramount for applications. For example, size homogeneity is highly desired for photonic applications of semiconductor quantum dots [1] and nanowires [2]. Consequently, a considerable effort has been made to narrow up the size distribution (SD) of nanostructures by various means [3–21]. Unfortunately, theories of surface nucleation with a fixed critical size [22,23] (hereafter referred to as regular growth) or macroscopic nucleation with a time-dependent critical size [24,25] show that the SDs usually tend to broaden due to the random character of nucleation and fluctuation-induced effects [25]. Suppression of this broadening has been demonstrated for the Stranski-Krastanow GeSi and InGaAs quantum dots. A complex interplay between the elastic stress relaxation, time-dependent wetting layer thickness, surface or edge energy constraints, elastic interactions through the substrate, and shape transformations in quantum dot ensembles may result in the kinetic narrowing of their SDs under appropriate growth conditions [5–7,9–15]. Of course, one can use epitaxial growth on prepatterned substrates in order to improve the size and spatial uniformity, as in Ref. [8] in the case of Ge nanoislands on Si(100). Despite many efforts, however, the quantum dot arrays rarely achieve truly deltalike SD shapes. Other examples include Au-catalyzed Ge nanowires whose length converges to a certain one but only at a given moment of time [19] or self-induced GaN nanowires with the length distribution narrowing due to wire-to-wire reemission of gallium [21].

Here, we consider one important case of one-dimensional nanostructures of a binary material where the axial growth rate is determined by the vapor flux of one element and the radial growth rate is given by the difference between the vapor plus diffusion flux of the other element and the axial growth rate. This growth picture is observed in vapor-liquid-solid (VLS) growth of III-V nanowires catalyzed by liquid droplets of a group III metal [25–30] and has recently been shown to yield a specific self-equilibration effect on the nanowire radii [31–33]. More generally, our model applies when a size-dependent regular growth rate can be either positive for all sizes or change its sign from positive to negative depending on the external conditions. This is an inverted situation compared to standard growth theories where the growth rate is positive for all sizes in regular growth [22,23] or changes from negative to positive at a critical size in nucleation theory [24,25]. Prior works studied only individual nanowires [31,33] or the deterministic first-order equation for the SD (neglecting kinetic fluctuations) [32]. Consequently, our goal is to calculate explicitly the SD based on the second-order Fokker-Planck equation and to show how Poissonian broadening can be completely suppressed and the desired size uniformity achieved by tuning the vapor environment.

## II. GOVERNING EQUATION AND ITS SOLUTION

Consider an ensemble of nanostructures described by the rate equations for the discrete SD $f_r(\tau)$ over the size $r$ at time $\tau$,

$$\frac{df_r(\tau)}{d\tau} = W_{r-1}^{+} f_{r-1}(\tau) + W_{r+1}^{-} f_{r+1}(\tau) - (W_r^{+} + W_r^{-}) f_r(\tau). \tag{1}$$

For simplicity, the attachment and detachment rates $W_r^{+}$ and $W_r^{-}$ are assumed independent of $\tau$. The continuum approximation to Eq. (1) at $r \gg 1$ has the form of the Fokker-Planck equation

$$\frac{\partial f(r,\tau)}{\partial \tau} = -\frac{\partial}{\partial r}[A(r) f(r,\tau)] + \frac{1}{2}\frac{\partial^2}{\partial r^2}[B(r) f(r,\tau)]. \tag{2}$$

The kinetic coefficients

$$A(r) = W_r^{+} - W_r^{-}, \quad B(r) = W_r^{+} + W_r^{-} \tag{3}$$

describe the deterministic growth rate and kinetic fluctuations, respectively. Writing $\partial^2[Bf]/\partial r^2$ or $\partial[B\partial f/\partial r]/\partial r$ in Eq. (2) is equivalent for small enough $dB/dr$ [25].

Since both $W_r^{+}$ and $W_r^{-}$ are positive, the $B(r)$ term is always positive while the deterministic growth rate $dr/d\tau = A(r)$ can be of either sign. The $A(r)$ term is positive for all $r$ in

*dubrovskii@mail.ioffe.ru

 

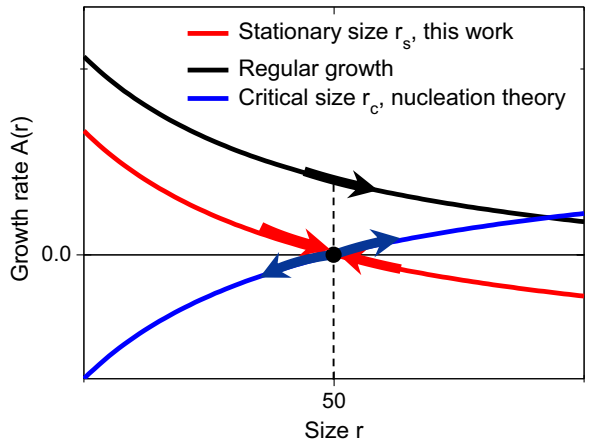


FIG. 1. Chart schematizing possible growth scenarios with the stationary size (attractive point $r_s = 50$), regular growth, and the critical size (repulsive point $r_c = 50$).

regular growth [22,23], while in nucleation theory it changes from negative to positive at the critical size $r_c$ (generally, this $r_c$ is time dependent) [24,25]. In the latter case, the system is unstable—large nuclei with $r > r_c$ will grow and smaller nuclei with $r < r_c$ decay. This gives rise to phase separation via nucleation and the growth of stable supercritical nuclei. For the Stranski-Krastanow quantum dots [4–14] or, more generally, three-dimensional islands on a lattice mismatching substrate [25,34], the growth of large enough islands can be suppressed by several factors, including the hut-to-dome shape transformation in GeSi systems or strain-induced barriers for the adatom attachment. In this case, the Gibbs energy for island formation reaches its maximum at a critical size and a minimum at a certain stationary size $r_s$, leading to a self-limiting growth from $r_c$ to $r_s$ [11,34].

Later on in this paper, we consider a simplified situation where the deterministic growth rate can be tuned from positive for all $r$, as in regular growth, to changing its sign from positive to negative at the stationary size $r_s$. Examples of such self-stabilized growth will be given in the next section. Clearly, nanostructures are expected to grow infinitely when $A(r)$ is positive and converge to the stationary size when $A(r)$ changes its sign at $r_s$ in such a way that smaller nanostructures swell and larger nanostructures shrink to $r_s$ at $\tau \to \infty$. The three possible scenarios are illustrated in Fig. 1. Our aim is to find explicitly the SD shapes in the infinite versus self-stabilized growth and to show quantitatively how the SDs broaden or narrow up depending on the sign of $A(r)$.

According to Refs. [35–37], the SD treatment is considerably simplified by rearranging Eq. (2) in terms of the "invariant size" $\rho$ defined as

$$\frac{d\rho}{dr} = \frac{1}{A(r)}, \quad \rho(r=0) = 0. \tag{4}$$

The $\rho$ variable starts from zero at $r = 0$ and tends to infinity at $r \to \infty$ in regular growth [provided that $A(r)$ does not increase faster than $r$ for large $r$] or at $r \to r_s$ in self-stabilized growth. Introducing the SD $g(\rho,\tau)$ by the definition

$$g(\rho,\tau) = |A(r)| f(r,\tau), \tag{5}$$

Eq. (2) modifies to

$$\frac{\partial g(\rho,\tau)}{\partial \tau} = -\frac{\partial g(\rho,\tau)}{\partial \rho} + \frac{1}{2}\frac{\partial^2}{\partial \rho^2}[F(\rho) g(\rho,\tau)], \tag{6}$$

with

$$F(\rho) = \frac{B(r)}{A^2(r)} = \frac{W_r^+ + W_r^-}{(W_r^+ - W_r^-)^2}. \tag{7}$$

The negative sign of the regular growth rate in Eq. (6) for $A(r)$ of either sign is ensured by the absolute value of $A(r)$ taken in Eq. (5), while the fluctuation term $F(\rho)$ is insensitive to the sign of $A(r)$. It is easy to see that the mean value of $\rho$ evolves in time according to $d\langle\rho\rangle/d\tau = 1$ and hence

$$\langle\rho\rangle = \rho_0 + \tau. \tag{8}$$

Neglecting the dispersion of the SD in the term with the second derivative in Eq. (6), we can write approximately

$$\frac{\partial g}{\partial \langle\rho\rangle} = -\frac{\partial g}{\partial \rho} + \frac{F(\langle\rho\rangle)}{2}\frac{\partial^2 g}{\partial \rho^2}. \tag{9}$$

This equation has the Gaussian solution [35–37]

$$g(\rho,\langle\rho\rangle) = \frac{1}{\sqrt{2\pi\psi(\langle\rho\rangle)}} \exp\left[-\frac{(\rho - \langle\rho\rangle)^2}{2\psi(\langle\rho\rangle)}\right]. \tag{10}$$

Here, the variance $\psi(\langle\rho\rangle)$ is obtained as a solution to the equation

$$\frac{d\psi}{d\langle\rho\rangle} = F(\langle\rho\rangle), \quad \psi(\langle\rho\rangle = \rho_0) = \psi_0. \tag{11}$$

Of course, this result applies only if the initial SD at $\tau = 0$ can be presented in the form given by Eq. (10) with a certain mean size $\rho_0$ and variance $\psi_0$.

## III. PARTICULAR MODEL

Figure 2 shows a binary III-V nanowire with a liquid droplet on top, grown by the VLS method [38]. The catalyst droplet can be either gold or a group III metal, but in many cases of gold-assisted growth the liquid alloy has a high concentration of group III atoms [25]. On the other hand, the concentration of highly volatile group V atoms in the droplet is always very low. Whenever the alloy is group III rich, the VLS axial growth rate $dl/dt$ is group V limited and often simply given by the group V vapor flux $v_5$ [26,39,40]. Thus, the mean nanowire length gives a linear measure of time $t$ and we can define our $\tau$ as $\tau = v_5 t = \langle l\rangle$. Furthermore, if we neglect a specific effect of nucleation antibunching [41–45] on the length distribution of nanowires, the latter is given by [44]

$$f(l,\langle l\rangle) = \frac{1}{\sqrt{2\pi\langle l\rangle}} \exp\left[-\frac{(l - \langle l\rangle)^2}{2\langle l\rangle}\right]. \tag{12}$$

As shown in Ref. [46], this Poissonian broadening is the best case regarding the length uniformity—when nanowires grow by surface diffusion, the length distribution is much broader.

The droplet seated on the nanowire top is a nonstationary reservoir of group III atoms. Therefore, the random variable of interest is the dimensionless radius of the droplet base $r$, which defines the time-dependent (or $\langle l\rangle$-dependent) radius of

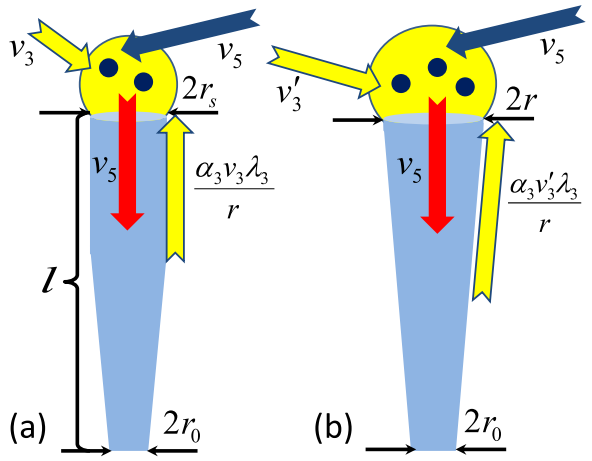


FIG. 2. Binary III-V nanowires growing from a group III rich alloy droplet (e.g., GaAs nanowire growing from Ga droplet with a low concentration of As) with the vapor fluxes $v_3$, $v_5$ and the effective diffusion length of the group III adatoms $\lambda_3$; $l$ and $r$ are the nanowire length and top radius in the units of lattice spacing. The elongation rate $v_5$ is determined by the vapor flux on a nondiffusive group V element and equals the group III sink from the droplet. At a low group III influx $v_3$, the diffusion flux of the group III adatoms from the nanowire sidewalls compensates a negative III/V influx imbalance and leads to self-stabilized radial growth to the stationary radius of the nanowire top $r_s$, regardless of the initial droplet size $r_0$, as in (a). Increasing $v_3$ yields the transition to regular radial growth where the nanowire top radius increases all the way, as in (b).

the nanowire top. The droplet size increases when the group III atom is brought from a vapor or by surface diffusion and decreases when the group III atom crystallizes into a III-V pair at the liquid-solid interface under the droplet. Assuming a stationary group V concentration inside the droplet [39], the crystallization rate equals the group V vapor flux $v_5$. The radial growth rate at the nanowire top is given by [32]

$$\frac{dr}{d\langle l\rangle} = \varepsilon\left(\frac{v_3}{v_5} + \alpha_3\frac{v_3}{v_5}\frac{\lambda_3}{r} - 1\right), \tag{13}$$

showing that the nanowire top radius changes with the mean length over the ensemble of nanowires. Here, $\varepsilon \ll 1$ is a time-independent shape constant (under the assumption of a fixed droplet shape), $v_3$ is the vapor flux of the group III element, $\alpha_3$ is a geometrical factor, and $\lambda_3$ is the diffusion length of the group III adatoms on the nanowire side facets [25,47], as illustrated in Fig. 2. The kinetic coefficients in Eqs. (1) and (2) are defined as

$$W_r^+ = \varepsilon\left(\frac{v_3}{v_5} + \alpha_3\frac{v_3}{v_5}\frac{\lambda_3}{r}\right), \quad W_r^- = \varepsilon, \tag{14}$$

$$A(r) = a + \frac{b}{r}, \quad B(r) = c + \frac{b}{r}, \tag{15}$$

with $a = \varepsilon[(v_3/v_5) - 1]$, $b = \varepsilon\alpha_3(v_3/v_5)\lambda_3$, and $c = \varepsilon[(v_3/v_5) + 1]$. The $b$ and $c$ values are always positive, while $a$ is positive at $v_3 > v_5$ and negative at $v_3 < v_5$. The radial growth is infinite when $a > 0$ and stabilizes to $r_s = -b/a$ when $a < 0$.

Thus, the transition from infinite to self-stabilized radial growth is regulated simply by the V/III flux ratio [31–33]. For a given $v_5$ and $\lambda_3$, self-stabilized radial growth to $r_s$ occurs at lower $v_3$ [Fig. 2(a)] while at higher $v_3$ the nanowire top radius will continue increasing [Fig. 2(b)]. Without vapor-solid growth at the nanowire sidewalls, this transition will also lead to the shape transformation from straight nanowires with a tapered bottom to reverse tapered nanowires all the way, as illustrated in Fig. 2. If the nanowires are able to maintain a cylindrical shape by step flow on their sidewalls [48,49], we will observe straight nanowires whose radius either becomes homogeneous regardless of the initial droplet SD [32] or swell in the course of growth [30,31].

More generally, the model $A(r) = a + b/r^\alpha$ applies when the growth rate of a nanoparticle contains a sign alternating size-independent term (adsorption-desorption term or chemical reaction) and a positive size-dependent term (diffusion). The simplest system of this kind would be a nanoparticle growing on a substrate from the vapor flux which is smaller than the desorption rate, and a positive diffusion-induced term. Three-dimensional nanoislands in lattice-mismatched material systems such as the Stranski-Krastanow semiconductor quantum dots [4–15] will also exhibit self-equilibration provided that the growth rate of large islands is suppressed and that this effect does not lead to secondary nucleation [11,34]. Such regimes are anticipated when $r_s \gg r_c$ and, on the other hand, the critical size $r_c$ remains large enough to disable nucleation from the wetting layer or the adatom sea at a later growth stage. In what follows, the SD treatment is presented in terms of the radius distributions of self-catalyzed III-V nanowires, but the results can easily be reformulated for other material systems exhibiting the size self-equilibration as described above.

Following the general procedure, integration of Eq. (4) with $A(r)$ given by Eq. (15) readily yields

$$\rho = \frac{r}{a} - \frac{b}{a^2}\ln z(r), \quad z(r) = 1 + \frac{ar}{b}. \tag{16}$$

Equation (8) shows that

$$\langle\rho\rangle = \rho_0 + \langle l\rangle, \tag{17}$$

where we can use Eq. (16) for $\rho_0$ at $r = r_0$. From Eqs. (7) and (15) we get

$$F(r) = \frac{c + b/r}{(a + b/r)^2}. \tag{18}$$

According to Eq. (11), the variance of the Gaussian SD in terms of the $\rho$ variable should be obtained from the equation $d\psi/d\langle l\rangle = F(\langle l\rangle)$, with $\psi(\langle l\rangle = 0) = \psi_0$. We now introduce the $r_*$ variable by definition $dr_*/d\langle l\rangle = a + b/r_*$ with $r_*(\langle l\rangle = 0) = 0$, which is equivalent to

$$\langle l\rangle = \frac{r_*}{a} - \frac{b}{a^2}\ln z(r_*). \tag{19}$$

Using $d\psi/d\langle l\rangle = (a + b/r_*)d\psi/dr_*$, we arrive at

$$\frac{d\psi}{dr_*} = \frac{c + b/r_*}{(a + b/r_*)^3}, \quad \psi(r_* = 0) = \psi_0. \tag{20}$$

Integration of this gives

$$\psi(r_*) = \psi_0 + \frac{1}{a^4}\left[acr_* - b(3c-a)\ln z(r_*) - b(3c-2a)\left(\frac{1}{z(r_*)}-1\right) + \frac{b(c-a)}{2}\left(\frac{1}{z^2(r_*)}-1\right)\right]. \quad (21)$$

Combining Eqs. (5), (10), (16), (17), and (19) yields our final result for the SD in the form

$$f(r,r_*) = \frac{r}{b|z(r)|}\frac{1}{\sqrt{2\pi\psi(r_*)}}\exp\left[-\frac{y^2(r,r_*)}{2\psi(r_*)}\right], \quad (22)$$

with

$$y(r,r_*) = \frac{r-r_0-r_*}{a} - \frac{b}{a^2}\ln\left[\frac{z(r)}{z(r_0)z(r_*)}\right]. \quad (23)$$

This $y$ can be presented equivalently as

$$y = \frac{r-r_m}{a} - \frac{b}{a^2}\ln\left[\frac{z(r)}{z(r_m)}\right]. \quad (24)$$

Here, $r_m$ is the most representative radius in the distribution which equals $r_0$ at $\langle l\rangle = 0$:

$$\langle l\rangle = \frac{r_m - r_0}{a} - \ln\left[\frac{z(r_m)}{z(r_0)}\right]. \quad (25)$$

As mentioned earlier, our solution is valid only when the initial SD can be approximated by Eqs. (21)–(23) with $r_* = 0$. In self-stabilized regime, this requires $r_0$ to be much smaller or greater than $r_s$. Otherwise, the solution given by Eqs. (19) and (21)–(23) with $r_0 = 0$ and $\psi_0 = 0$ define the Green's function which should be convoluted with the initial condition $f_0(r_0)$ to find the time evolution of the SD.

## IV. RESULTS AND DISCUSSION

We first analyze the Poissonian case in the absence of surface diffusion ($b = 0$) in which the nanostructures grow infinitely when $a > 0$. Equations (21)–(24) are reduced to

$$f(r,\langle r\rangle) = \frac{1}{\sqrt{2\pi[D_0 + (c/a)(\langle r\rangle - r_0)]}} \times \exp\left[-\frac{(r-\langle r\rangle)^2}{2[D_0 + (c/a)(\langle r\rangle - r_0)]}\right]. \quad (26)$$

Here, $\langle r\rangle = r_0 + a\langle l\rangle$ is the mean radius and $D_0 = \psi_0 a^2$ is the variance of the Gaussian SD of droplets with the mean radius $r_0$. Therefore, the mean radius scales linearly with the mean length and the variance scales linearly with the mean radius with the prefactor $c/a = (v_3 + v_5)/(v_3 - v_5)$. Hence, the broadening of the SD becomes larger for a smaller difference $v_3 - v_5$.

When surface diffusion is enabled ($b > 0$), the system behavior is determined by the sign of $a$. Under group III rich conditions ($v_3 > v_5$, $a > 0$), all droplets grow infinitely, regardless of their initial sizes, as shown by the curves in Fig. 3 for the model parameters $a = 0.01$ and $b = 5$. However, the growth rates are different—Fig. 3 shows that the nanostructures having a smaller initial radius of 60 grow faster and that the $r_m(\langle l\rangle)$ correlation is nonlinear, while the nanostructures with $r_0 = 150$ grow slower and the $r_m(\langle l\rangle)$ dependence becomes almost linear. Figure 4 shows how the initially narrow SDs broaden with time, similarly to Refs. [35,44,50].

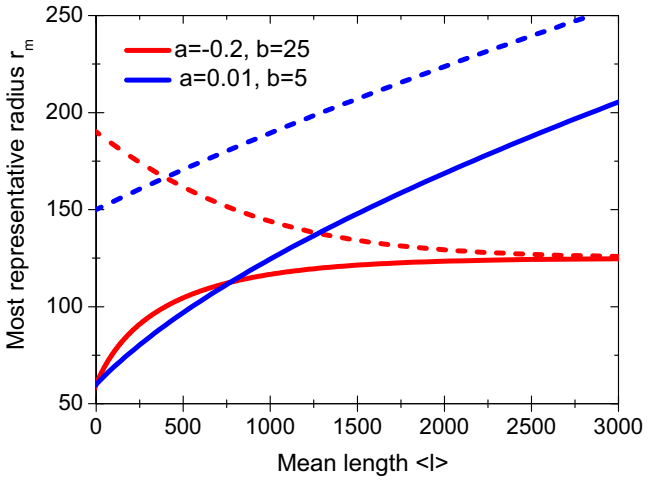


FIG. 3. The most representative radius in the SDs vs the mean length in the regimes of infinite growth ($a = 0.01$, $b = 5$) and radius self-stabilization to $r_s = 125$ ($a = -0.2$, $b = 25$) for two different initial conditions: $r_0 = 60$ in both regimes (solid lines), $r_0 = 190$ in self-stabilized growth, and $r_0 = 150$ in infinite growth (dashed lines).

Under group V rich conditions ($v_3 < v_5$, $a < 0$), the most representative size in the SDs self-equilibrates to $r_s$ regardless of the initial condition, as in Ref. [32]. The corresponding curves in Fig. 3 at $a = -0.2$ and $b = 25$ show how small nanostructures swell and large nanostructures shrink to reach the stationary size. An analysis of Eqs. (19) and (21)–(23) in a self-stabilized regime shows that $r_*$ always remains smaller than $r_s$ and asymptotically tends to $r_s$. The nanostructures emerging from large droplets will never become smaller than $r_s$, while smaller nanostructures will never grow larger than $r_s$. In the asymptotic stage, the variance $\psi$ tends to

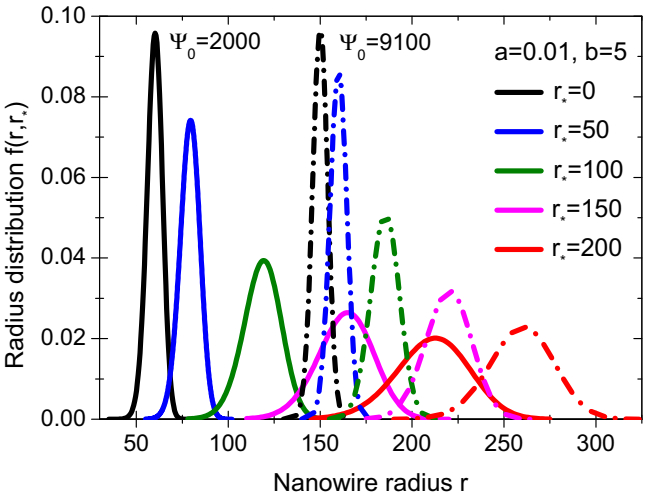


FIG. 4. Broadening of the SDs in the case of infinite growth for $r_0 = 60$, $\psi_0 = 2000$ (solid lines) and $r_0 = 150$, $\psi_0 = 9100$ (dashed-dotted lines); other parameters are the same as in Fig. 3.

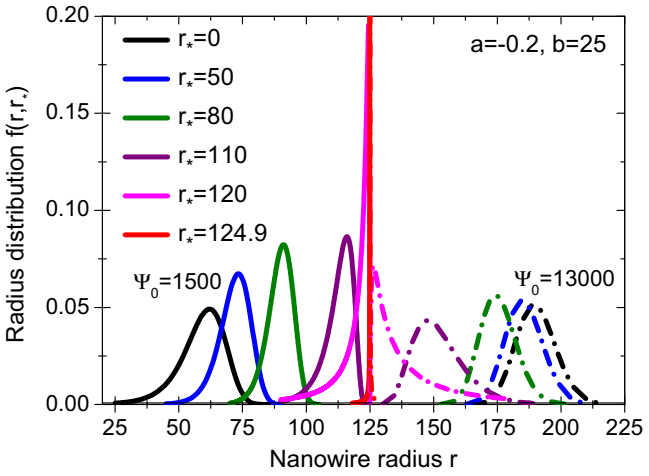


FIG. 5. Narrowing of the SDs in the case of self-stabilized growth for $r_0 = 60$, $\psi_0 = 1500$ (solid lines) and $r_0 = 190$, $\psi_0 = 13\,000$ (dashed-dotted lines); other parameters are the same as in Fig. 3.

infinity faster than $y^2$ and hence the exponential term in Eq. (22) tends to one. The limiting behavior of the SD in thus determined by the preexponential factor which scales as $[\pi b(c-a)]^{-1/2} r_s^2 (r_s - r_*)/|r_s - r|$. This combination tends to zero when $r_* \to r_s$ for almost all $r$ except for a narrow region of radii that are only slightly smaller or larger than $r_s$ (depending on whether the initial size $r_0$ was smaller or larger than $r_s$). At $r \to r_s$, the maximum of the SD is much larger than one due to $r_s \gg 1$. Therefore, the SD narrows up regardless of the initial conditions to an asymmetric monodispersive shape, as shown in Fig. 5 for the two initial SDs with $r_0 = 60$, $\psi_0 = 1500$ and $r_0 = 190$, $\psi_0 = 13\,000$.

In summary, we have developed a model that reveals an interesting possibility for narrowing the SDs of different nanostructures. The narrowing effect is observed when a sign alternating growth rate changes from positive to negative as the size increases. The model applies to self-catalyzed VLS III-V nanowires and may also work for other systems. Within certain approximations, the analytic SD has been obtained in the form of a modified Gaussian distribution with a size-dependent prefactor. This solution describes both Poissonian broadening and kinetic narrowing of the SD depending on the growth parameters. Overall, the obtained results can be used for setting appropriate conditions that result in the kinetic narrowing of the SDs in different material systems.

## ACKNOWLEDGMENT

The author gratefully acknowledges financial support from the Russian Science Foundation under Grant No. 14-22-00018.

[1] S. Fafard, K. Hinzer, S. Raymond, M. Dion, J. McCaffrey, Y. Feng, and S. Charbonneau, Science **274**, 1350 (1996).
[2] O. L. Muskens, S. L. Diedenhofen, B. C. Kaas, R. E. Algra, E. P. A. M. Bakkers, J. G. Rivas, and A. Lagendijk, Nano Lett. **9**, 930 (2009).
[3] J. Tersoff, C. Teichert, and M. G. Lagally, Phys. Rev. Lett. **76**, 1675 (1996).
[4] J. A. Floro, E. Chason, R. D. Twesten, R. Q. Hwang, and L. B. Freund, Phys. Rev. Lett. **79**, 3946 (1997).
[5] F. M. Ross, J. Tersoff, and R. M. Tromp, Phys. Rev. Lett. **80**, 984 (1998).
[6] G. Medeiros-Ribeiro, A. M. Bratkovski, T. I. Kamins, D. A. A. Ohlberg, and R. S. Williams, Science **279**, 353 (1998).
[7] C. Teichert, M. G. Lagally, L. J. Peticolas, J. C. Bean, and J. Tersoff, Phys. Rev. B **53**, 16334 (1996).
[8] Z. Zhong, A. Halilovic, T. Fromherz, F. Schäffler, and G. Bauer, Appl. Phys. Lett. **82**, 4779 (2003).
[9] V. A. Shchukin, N. N. Ledentsov, P. S. Kop'ev, and D. Bimberg, Phys. Rev. Lett. **75**, 2968 (1995).
[10] C. Chiu, Appl. Phys. Lett. **75**, 3473 (1999).
[11] A. V. Osipov, S. A. Kukushkin, F. Schmitt, and P. Hess, Phys. Rev. B **64**, 205421 (2001).
[12] P. Liu, Y. W. Zhang, and C. Lu, Phys. Rev. B **67**, 165414 (2003).
[13] P. Liu, Y. W. Zhang, and C. Lu, Phys. Rev. B **68**, 195314 (2003).
[14] P. Liu, Y. W. Zhang, and C. Lu, Phys. Rev. B **68**, 035402 (2003).
[15] V. G. Dubrovskii, G. E. Cirlin, and V. M. Ustinov, Phys. Rev. B **68**, 075409 (2003).
[16] K. Bromann, C. Felix, H. Brune, W. Harbich, R. Monot, J. Buttet, and K. Kern, Science **274**, 956 (1996).
[17] X. Peng, J. Wickham, and A. P. Alivisatos, J. Am. Chem. Soc. **120**, 5343 (1998).
[18] C. Ratsch, J. DeVita, and P. Smereka, Phys. Rev. B **80**, 155309 (2009).
[19] V. G. Dubrovskii, T. Xu, Y. Lambert, J.-P. Nys, B. Grandidier, D. Stievenard, W. Chen, and P. Pareige, Phys. Rev. Lett. **108**, 105501 (2012).
[20] J. P. Mastandrea, M. P. Sherburne, C. N. Boswell-Koller, C. A. Sawyer, J. Guzman, K. C. Bustillo, J. W. Ager III, E. E. Haller, and D. C. Chrzan, J. Appl. Phys. **114**, 234301 (2013).
[21] K. K. Sabelfeld, V. M. Kaganer, F. Limbach, P. Dogan, O. Brandt, L. Geelhaar, and H. Riechert, Appl. Phys. Lett. **103**, 133105 (2013).
[22] A. Venables, G. D. T. Spiller, and M. Hanbucken, Rep. Prog. Phys. **47**, 399 (1984).
[23] J. W. Evans, P. A. Thiel, and M. C. Bartelt, Surf. Sci. Rep. **61**, 1 (2006).
[24] D. Kashchiev, *Nucleation: Basic Theory with Applications* (Butterworth-Heinemann, Oxford, U.K., 2000).
[25] V. G. Dubrovskii, *Nucleation Theory and Growth of Nanostructures* (Springer, Heidelberg, 2014).
[26] C. Colombo, D. Spirkoska, M. Frimmer, G. Abstreiter, and A. Fontcuberta i Morral, Phys. Rev. B **77**, 155326 (2008).
[27] D. Rudolph, S. Hertenberger, S. Bolte, W. Paosangthong, D. Spirkoska, M. Doblinger, M. Bichler, J. J. Finley, G. Abstreiter, and G. Koblmuller, Nano Lett. **11**, 3848 (2011).
[28] S. G. Ghalamestani, A. M. Munshi, D. L. Dheeraj, B. O. Fimland, H. Weman, and K. A. Dick, Nanotechnology **24**, 405601 (2013).

[29] F. Matteini, G. Tütüncüoglu, H. Potts, F. Jabeen, and A. Fontcuberta i Morral, Cryst. Growth Des. **15**, 3105 (2015).
[30] F. Matteini, V. G. Dubrovskii, D. Rüffer, G. Tütüncüoğlu, Y. Fontana, and A. Fontcuberta i Morral, Nanotechnology **26**, 105603 (2015).
[31] G. Priante, S. Ambrosini, V. G. Dubrovskii, A. Franciosi, and S. Rubini, Cryst. Growth Des. **13**, 3976 (2013).
[32] V. G. Dubrovskii, T. Xu, A. Díaz Álvarez, S. R. Plissard, P. Caroff, F. Glas, and B. Grandidier, Nano Lett. **15**, 5580 (2015).
[33] J. Tersoff, Nano Lett. **15**, 6609 (2015).
[34] Y. Berdnikov, N. V. Sibirev, V. G. Dubrovskii, and J. H. Kang, J. Phys.: Conf. Ser. **643**, 012012 (2015).
[35] V. G. Dubrovskii, J. Chem. Phys. **131**, 164514 (2009).
[36] V. G. Dubrovskii and M. V. Nazarenko, J. Chem. Phys. **132**, 114507 (2010).
[37] V. G. Dubrovskii and N. V. Sibirev, Phys. Rev. B **89**, 054305 (2014).
[38] R. S. Wagner and W. C. Ellis, Appl. Phys. Lett. **4**, 89 (1964).
[39] F. Glas, M. R. Ramdani, G. Patriarche, and J. C. Harmand, Phys. Rev. B **88**, 195304 (2013).
[40] V. G. Dubrovskii, J. Cryst. Growth **440**, 62 (2016).
[41] C. Y. Wen, J. Tersoff, M. C. Reuter, E. A. Stach, and F. M. Ross, Phys. Rev. Lett. **105**, 195502 (2010).
[42] F. Glas, J. C. Harmand, and G. Patriarche, Phys. Rev. Lett. **104**, 135501 (2010).
[43] A. D. Gamalski, C. Ducati, and S. Hofmann, J. Phys. Chem. C **115**, 4413 (2011).
[44] V. G. Dubrovskii, Phys. Rev. B **87**, 195426 (2013).
[45] F. Glas, Phys. Rev. B **90**, 125406 (2014).
[46] V. G. Dubrovskii, Y. Berdnikov, J. Schmidtbauer, M. Borg, K. Storm, K. Deppert, and J. Johansson, Cryst. Growth Des. **16**, 2167 (2016).
[47] L. E. Fröberg, W. Seifert, and J. Johansson, Phys. Rev. B **76**, 153401 (2007).
[48] V. G. Dubrovskii, V. Consonni, L. Geelhaar, A. Trampert, and H. Riechert, Appl. Phys. Lett. **100**, 153101 (2012).
[49] V. G. Dubrovskii, V. Consonni, A. Trampert, L. Geelhaar, and H. Riechert, Phys. Rev. B **85**, 165317 (2012).
[50] V. G. Dubrovskii and M. V. Nazarenko, J. Chem. Phys. **132**, 114508 (2010).